High Voltage Pulsed Atmospheric Pressure Helium Plasma Jet

G.M.El-Aragi

Plasma Physics and Nuclear Fusion Dept., Nuclear Research Center, AEA, PO 13759 Cairo, Egypt

Abstract

Non-equilibrium cold plasma jets generated under atmospheric pressure by means of high voltage pulsed power generator are extended up to a few centimeters long in the surrounding air. The generator is consisting of a negative dc source, a Blumlein-type pulse-forming network (E-PFN), and a dynamic spark gap switch. The plasma jet generated by the device using helium as the operating gas depends on the applied voltage and the gas flow rate. It is found that the plasma jet width and the radiant intensity depend on the discharge current.

Introduction

Non-thermal plasmas are frequently called,"non-equilibrium" plasmas because they are characterized by a large difference in the temperature of the electrons relative to the ions and neutrals. Since the electrons are extremely light, they move quickly and have almost no heat capacity. In these plasmas, $T_e >> T_i \approx T_n$. Ionization is maintained by the impact of electrons (which may have temperatures ranging from 0.1 to more than 20 eV) with neutral species, producing additional electrons and ions. These plasmas are typically maintained by the passage of electrical current through a gas.

Atmospheric pressure non-equilibrium plasmas have become powerful experimental tools for many applications in areas such as micro fabrications in microelectronics [1], surface modifications [2], light sources [3-4], and environmental processing [5].

Cold atmospheric pressure plasma jet devices have recently attracted significant attention [6-7]. The most important devices for generating atmospheric pressure non-thermal plasmas can be considered: atmospheric pressure plasma jet [8-9], plasma needle [10], plasma pencil [11-12], miniature pulsed glow-discharge torch [13], one atmosphere uniform glow-discharge plasma [14], resistive barrier discharge [15] and dielectric barrier discharge [16].

Experimental Setup

Fig. 1 shows the schematic diagram of the pulsed power generator used in this paper. The generator is consisting of a negative dc source, a Blumlein-type pulse-forming network (E-PFN), and a dynamic spark gap switch. A triggered spark gap switch was used as a closing switch of E-PFN. E-PFN had 4 stages of LC ladder, which were composed of 5 nF of capacitor and 3 μH of inductor. The characteristic impedance ($2\sqrt{L/C}$) and the pulse width ($2N\sqrt{LC}$) of E-PFN, calculated from capacitance (C) and inductance (L) of the LC ladder, and number (N) of LC ladder stages were approximately 49Ω and 1.0 μs, respectively.

A charging resistance value of 50kΩ is chosen in the present case which corresponds to a charging RC time constant of 1 ms, which is 40 times faster compared to the repetition rate of the pulse.

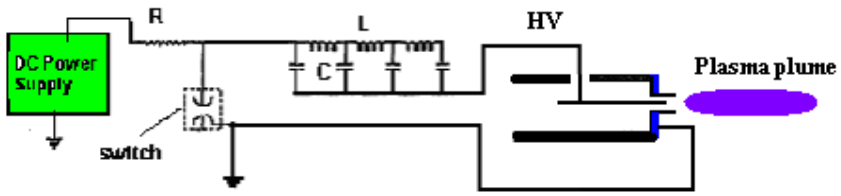

Fig.1. Schematic diagram of the pulsed power generator.

The high voltage (HV) wire electrode, which is made of a copper wire, is inserted into a hollow barrel of a syringe. The distance between the tip of the HV electrode and the nozzle is 0.5 cm.
When HV pulsed dc voltage (amplitudes up to 25 kV, repetition rate up to 25 Hz), applied to the HV electrode and helium gas was injected into the hollow barrel. This device made using medical syringe (made out of an insulating material cylinder). The gas was fed into the system via flow meter (OMEGA model). The applied voltage to and the discharge current through the discharge chamber were measured using a voltage divider (Home made), which was connected between the two electrodes, and a current monitor, which can be located upon returning to the ground. The signals from the voltage divider and the current monitor were recorded in a digitizing oscilloscope (Lecroy, USA) with a 200-MHz bandwidth.

Results and Discussion

The high voltage pulses are applied between the needle electrode positioned inside a dielectric cylinder (a simple medical syringe) and a metal ring placed on the exterior of this cylinder. In order to obtain electric discharges at atmospheric pressure, a high voltage pulses (tens of kV) which have limited duration (hundreds of nanoseconds) and are repeated (tens of pulses per second), in addition to an inert gas (helium) is introduced in the cylinder. The gas flows were in the range 0.5–10 l/min. The discharge takes place between the metallic needle top and a metallic ring fit on the outer surface of the syringe. Under optimal conditions, plasma is emitted as centimeter-long jets, just millimeters in diameter or even smaller.
The working gases are supplied by high-pressure cylinders. Gas pressure regulators are used to reduce the pressure of gases to a workable level. Then, gas flow controllers deliver the gases with the desired flow. For voltage amplitudes of 15–18 kV, the plasma jet is very weak. The plasma jet disappears for voltage amplitudes lower than 15 kV.
When helium is injected from the gas inlet and high voltage pulses 26 kV voltage is applied to the electrode, the plasma jet is generated and a plasma plume reaching length of 21 mm is launched through the end of the tube and in the surrounding air. The plasma has a cylindrical shape. The length of the plasma plume can be adjusted by the gas flow rate and the applied voltage.
A Lecroy 200 MS/s 4-channel digital storage oscilloscope model (9304c) was used to recorded voltage and current waveforms, via a high voltage probe and a pulse current transformer, respectively; and to calculate the discharge power. The measured peak value of the discharge current was approximately 10.5 A during the pulse. Fig. 2 shows the current and voltage waveforms measured as a function of time at an input energy of 6.76 J (maximum applied voltage 26 kV). Fig. 5 shows the power input as a fuunction of time, the maximum power approximately 150 kW at time 167 ns.

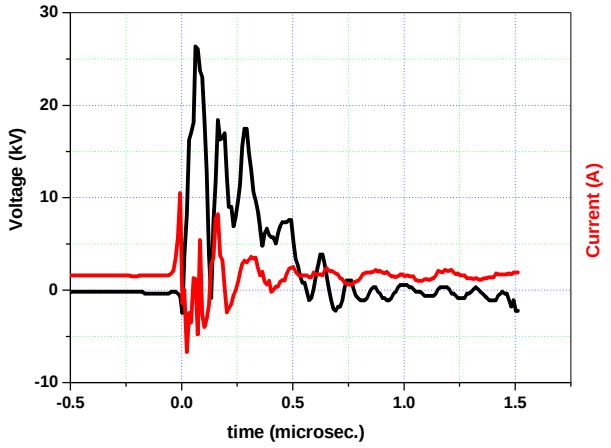

Fig. 2. Typical discharge current and the voltage waveforms.

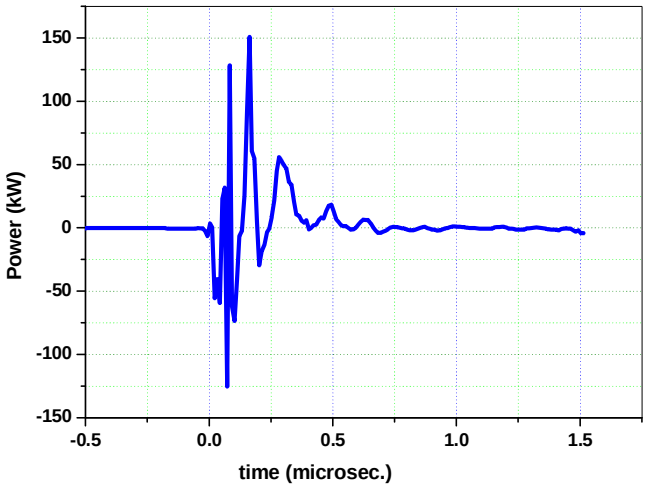

Fig 3. The power waveform of the device.

Figs (4 and 5) show the photographs of the plasma jet when helium gas was used as the carrier gas with different flow rate and applied voltage.

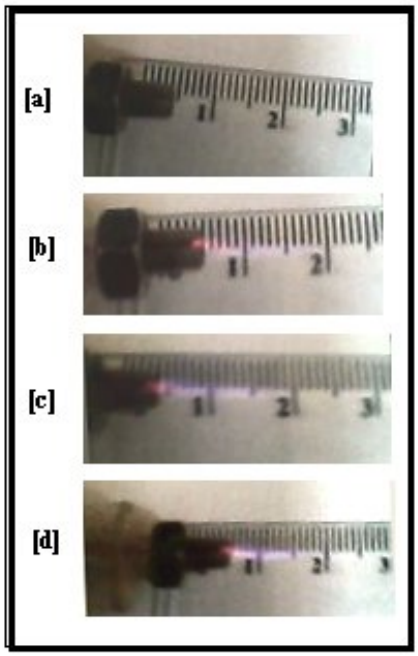

Fig. 4. Photographs of the jet when helium gas was used as the carrier gas, the radiant intensity increased with increasing discharge voltage minimum intensity at 18 kV [a] and maximum at 25 kV [d].

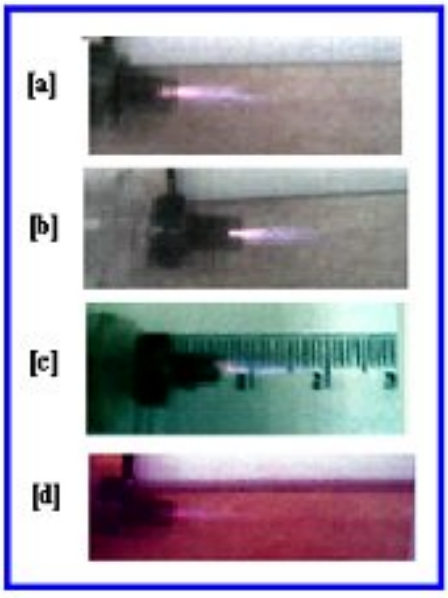

Fig. 5. Photographs of the jet when helium gas was used as the carrier gas, width of the plasma jet increased with increasing flow rate minimum width at 2 lpm [d] and maximum at 8 lpm [a].

Fig. 6. indicates the dependence of radiant intensity of plasma jet on discharge voltage.

As the result with decreasing discharge voltage, the width of the plasma jet became small.

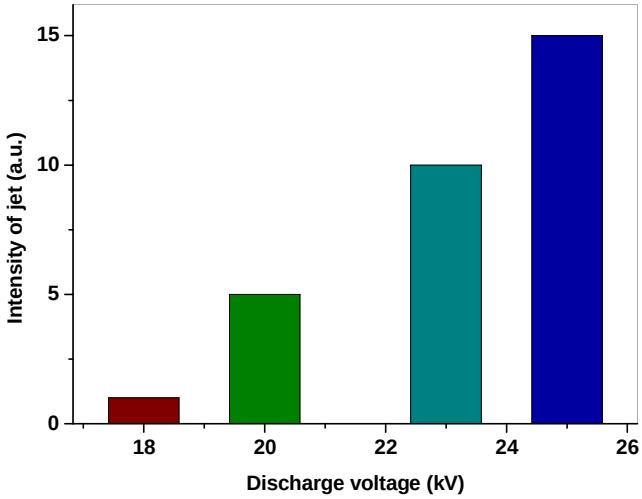

Fig. 6 Dependence of radiant intensity of plasma jet on discharge voltage.

Fig. 7 indicates the dependence of the plasma jet width on helium flow rate, the minimum width at 2 lpm and maximum at 8 lpm. With increase gas flow rate, discharge voltage increased. This is because a higher energy is necessary to get larger amounts of gas into excited states.

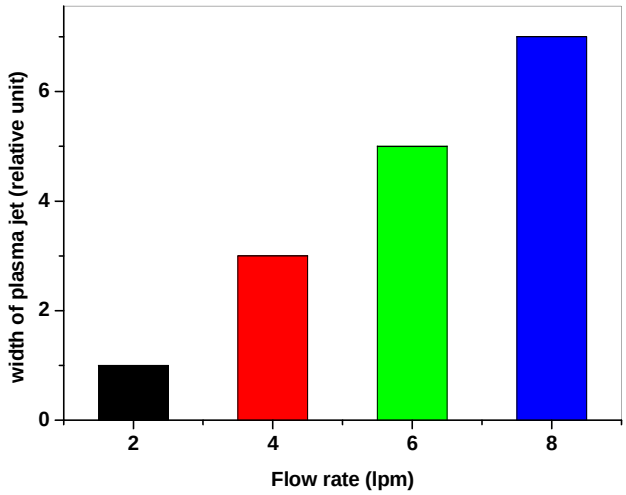

Fig. 7 Dependence of the plasma jet width on helium flow rate.

Conclusion

With increasing discharge current, the plasma jet width became more wider and the radiant intensity also increased with increasing gas flow rate. The discharge voltage increases with increasing in gas flow rate.

References

[1] R. M. Shakaran and K. P. Giapis, Appl. Phys. Lett. 79, 593 (2001).
[2] J. Benedikt, K. Focke, A. Yanguas-Gil, and A. von Keudell, Appl. Phys. Lett. 89, 251504 (2006).
[3] S. J. Park, K. S. Kim, and J. G. Eden, Appl. Phys. Lett. 86, 221501 (2005).
[4] A. Rahman, A. P. Yalin, V. Surla, O. Stan, K. Hoshimiya, Z. Yu, E. Littlefielc, and G. J. Collins, Plasma Sources Sci. Technol. 13, 537 (2004).
[5] K. Hensel, S. Katsura, A. Mizuna, IEEE Trans. Plasma. Sci. 33, 574 (2005).
[6] G. Li, H. Li, L. Wang, S. Wang, H. Zhao, W. Sun, X. Xing, and C. Bao, Appl. Phys. Lett. 92, 221504 (2008).
[7] J. Goree, B. Liu, D. Drake, and E. Stoffels, IEEE Trans. Plasma Sci. 34, 1317 (2006).
[8] A. Schutze, J.Y. Jeong, S.E. Babayan, J. Park, G.S. Selwin, R. F. Hicks, *IEEE Trans. Plasma Sci.* 26 (1998)1685.
[9] K. Niemi, Sh. Wang, V. Schultz-von der Gathen, H.F. Dbele, *Poster Conference Frontiers on Low Temperature Plasma Diagnostics* 2003 Lecce Italy, Available online: http://fltpd-5.ba.cnr.it/Paper/Libro/239.pdf
[10] E. Stoffels, A.J. Flikweert, W.W. Stoffels, G.M.W Kroesen, *Plasma Sources Sci. Technol.* 11 (2002) 383.
[11] J. Janca, L. Zajickova, M. Klima, P. Slavicek, *Plasma Chem. Plasma Proc.* 21 (2001) 565.
[12] M. Laroussi, C. Tendero, X. Lu, S. Alla, W.L. Hynes, *Plasma Process. Polym.* 3 (2006) 470.
[13] V. Léveillé, S. Coulombe, *Plasma Sources Sci. Technol.* 14 (2005) 467.
[14] J.R. Roth, D.M. Sherman, R. Ben Gadri, F. Karakaya, Z. Chen, T.C. Montie, K. Kelly-Winterberg, P.P-Y. Tsai, *IEEE Trans. Plasma Sci.* 28 (2001) 56.
[15] M. Laroussi, I. Alexeff, J.P. Richardson, F.F. Dier, *IEEE Trans. Plasma Sci.* 30 (2002) 158.
[16] S. Kanazawa, M. Gogoma, T. Moriwaki, S. Okazaki, *J. Appl. Phys. D: Appl. Phys.* 21 (1988) 838.